Pergamon

Int. J. Solids Structures Vol. 34, No. 1, pp. 99–112, 1997

0020-7683/97 $15.00 + .00

0020-7683(95)00290-1

DIRECT DIFFERENTIATION FORMULATION FOR BOUNDARY ELEMENT SHAPE SENSITIVITY ANALYSIS OF AXISYMMETRIC ELASTIC SOLIDS

BOO YOUN LEE
Solids & Structures Team, R & D Center, Korea Heavy Industries & Construction Co., Ltd, P.O. Box 77, Changwon 641-792, Korea

(*Received* 25 *April* 1995; *in revised form* 27 *November* 1995)

Abstract—An efficient direct differentiation method by continuum approach is presented for the shape design sensitivity analysis of axisymmetric elastic solids. The method is purely based on the axisymmetric boundary integral equation formulation. A new boundary integral equation for sensitivity analysis is derived by taking material derivative to the same integral identity that was used in the adjoint method. As sensitivities in terms of the shape design variables are directly calculated by solving the new BIE, the singular boundary condition which may arise in the adjoint method is avoided in the present direct method.

To validate the theoretical formulation, numerical implementation is done for three examples. For a hollow disk and a thick-walled cylinder problem with analytic solution, the sensitivities by present method are compared with analytic sensitivities. For an example of a spherical vessel, being rather practical, the sensitivities are compared with those by finite differences. Copyright © 1996 Elsevier Science Ltd

INTRODUCTION

The shape optimization problem is to find the optimal structural shape minimizing an objective function under prescribed constraints. For the numerical shape optimization using the mathematical programming technique, the sensitivity of the state variables, e.g., displacements and stresses, with respect to the boundary shape has to be calculated. Because inaccurate prediction of the sensitivity may increase the number of iterations to be taken and result in a divergent solution, it is very important to analyze the sensitivity accurately and efficiently during each iteration step.

In this point of view, continuous research efforts have been given to the area of the shape design sensitivity analysis (SDSA) based on the finite element method (FEM) [for a survey, see the recent paper of Chen and Choi (1994)]. While the FEM has been used as a popular tool for the SDSA, the boundary element method (BEM) has appeared as an alternative to the FEM. It results from the fact that we can obtain a relatively more accurate boundary solution and moreover, remeshing is very convenient when using the BEM instead of the FEM for the shape optimization. For this reason, considerable efforts have been devoted to research on the SDSA using the boundary element method (BEM) and numerous papers have appeared [see, for survey, Burczynski (1993)]. Since Mota Soares *et al.* (1984) used the BEM only as a tool for the solution of state equations, a lot of researchers have devoted time to developing a general method of the SDSA, whose background is based on the boundary integral equation (BIE) or the BEM. Choi and Kwak (1988) and Lee and Kwak (1991, 1992) have developed an adjoint variable method based on the BIE formulation. They derived adjoint systems by taking material derivative [Haug *et al.* (1986)] to the integral identity obtained from the direct and indirect BIE. A direct differentiation method has been presented by Barone and Yang (1988, 1989) for two and three-dimensional elasticity problems and by Rice and Mukherjee (1990) for axisymmetric elasticity problems, where the shape sensitivities are directly obtained by solving a BIE for sensitivity calculation. To overcome the singular boundary condition problem that may occur in the adjoint method, Choi and Choi (1990) and Choi and Kwak (1990) have presented a direct method by differentiating the same integral identity that was used in the adjoint method. The above described methods belong to a continuum approach, where a complete sensitivity formulation is derived first and then discretization by boundary elements followed. Another direct method is an implicit differentiation by Kane and Saigal (1988), where the coefficient matrices formed by the discretized BIE are differentiated. Saigal *et al.* (1989) have applied the method to axisymmetric elasticity problem.

This paper presents the direct differentiation method of the SDSA as applied to the axisymmetric elasticity problem. The method of Choi and Kwak (1990) confined to the two-dimensional problem is extended to the axisymmetric problem and a new BIE for the SDSA is derived. Saigal *et al.* (1989) have dealt with the axisymmetric problem but have used the implicit differentiation method. The method of Rice and Mukherjee (1990) on the axisymmetric problem covers the direct differentiation approach but the present method is basically different from their one. Present work completes the concept of the unified adjoint and direct approach using the axisymmetric BIE formulation, where a boundary integral identity is derived from the direct and indirect BIEs and the material derivative is taken. From the same differentiated equation, the sensitivity formula can be derived by introducing the adjoint variables as described in the adjoint method of Lee and Kwak (1992) or a new BIE for the direct sensitivity calculation can be derived as presented in the current paper. In this unified approach, which of the two methods is to be selected will depend on the numbers of the design variables and the performance functions of the shape optimization problem.

The theoretical formulation is validated by a numerical implementation of three examples: a hollow disk and a thick-walled cylinder problem with analytic solution and a spherical pressure vessel problem. For the two examples with analytic solutions, the sensitivities by the present method are compared with the analytic sensitivities. For the hollow disk problem, the result is also compared with that from Saigal *et al.* (1989) using the implicit differentiation method. For the spherical pressure vessel problem without analytic solution, the sensitivities are compared with those by finite differences.

BIE FORMULATION

An axisymmetric elasticity problem is considered for an isotropic and homogeneous solid body of arbitrary shape. The body can be represented as shown in Fig. 1 using a cylindrical coordinate system. The domain Ω and boundary Γ are defined in the symmetric section on the (R, Z) plane. The position in this plane will be denoted by x or x_0. Coordinates of points x and x_0 are represented by (R, Z) and (R_0, Z_0), respectively. If the displacement vector is denoted by $\mathbf{u}(x) = \{u_R, u_Z\}$, then the strain and stress tensors are expressed as

$$\varepsilon_{ij}(\mathbf{u}) = \tfrac{1}{2}(u_{i,j}+u_{j,i}), \quad i,j = R, Z$$

$$\varepsilon_{\theta\theta}(\mathbf{u}) = \frac{u_R}{R}$$

$$\sigma_{ij}(\mathbf{u}) = \lambda\varepsilon_{kk}\,\delta_{ij}+2\mu\varepsilon_{ij}, \quad i,j = R, \theta, Z \tag{1}$$

where λ and μ represent Lame's constants. If we consider the case without the body forces, the equilibrium equation is given by

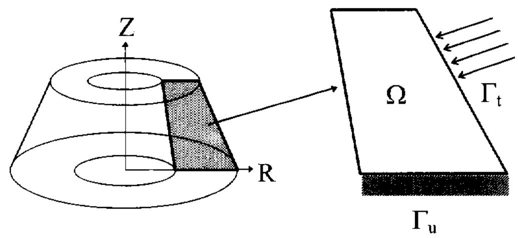

Fig. 1. An axisymmetric elasticity problem.

$$\sigma_{RR,R}(\mathbf{u})+\sigma_{RZ,Z}(\mathbf{u})+\frac{\sigma_{RR}(\mathbf{u})-\sigma_{\theta\theta}(\mathbf{u})}{R}=0$$

$$\sigma_{RZ,R}(\mathbf{u})+\sigma_{ZZ,Z}(\mathbf{u})+\frac{\sigma_{RZ}(\mathbf{u})}{R}=0. \tag{2}$$

A tensor notation is used from now on, with the indices representing an R or Z component. The boundary conditions are given on the boundary $\Gamma=\Gamma_u+\Gamma_t$ as

$$u_i(x)=u_{i0}(x),\quad x\in\Gamma_u$$

$$t_i(\mathbf{u})\equiv\sigma_{ij}(\mathbf{u})n_j(x)=t_{i0}(x),\quad x\in\Gamma_t \tag{3}$$

where n_i represents the outward unit normal vector and t_i the surface traction on the boundary. The displacement $u_{i0}(x)$ and surface traction $t_{i0}(x)$ are prescribed on Γ_u and Γ_t, respectively, as shown in Fig. 1.

Using the BIE formulation described in Lee and Kwak (1992), an integral identity is derived now for the axisymmetric elasticity problem. The problem can be formulated into the direct BIE by applying Somigliana's identity as follows [Bakr (1986), Banerjee and Butterfield (1981), Brebbia *et al.* (1984)]:

$$c_{ij}(x_0)u_j(x_0)=\int_\Gamma\{t_j(x)G_{ij}(x_0,x)-u_j(x)F_{ij}(x_0,x)\}R\,\mathrm{d}s,\quad x_0\in\Omega\cup\Gamma \tag{4}$$

where $\mathrm{d}s$ represents integration with respect to x along Γ, and $c_{ij}(x_0)$ is a function of the geometry of Γ. The kernels $G_{ij}(x_0,x)$ and $F_{ij}(x_0,x)$ are ring-type fundamental solutions for displacement and surface traction, respectively. Now, an arbitrary function ρ_i^* defined on the boundary can be introduced. For $x_0\in\Gamma$, eqn (4) can be transformed into the following equation by multiplying ρ_i^* and integrating over Γ as

$$\int_\Gamma u_j(x)\left\{c_{ij}(x)\rho_i^*(x)+\int_\Gamma\rho_i^*(x_0)F_{ij}(x_0,x)R_0\,\mathrm{d}s_0\right\}R\,\mathrm{d}s$$

$$-\int_\Gamma t_j(x)\int_\Gamma\rho_i^*(x_0)G_{ij}(x_0,x)R_0\,\mathrm{d}s_0R\,\mathrm{d}s=0 \tag{5}$$

where $\mathrm{d}s_0$ represents integration with respect to x_0 along Γ. On the other hand, an arbitrary axisymmetric system of displacement u_j^* and surface traction t_j^* may be considered, which can be expressed by the indirect BIE formulation [Banerjee and Butterfield (1981)] as

$$u_j^*(x)=\int_\Gamma\rho_i^*(x_0)G_{ij}(x_0,x)R_0\,\mathrm{d}s_0,\quad x\in\Omega\cup\Gamma$$

$$t_j^*(\mathbf{u}^*(x))=c_{ij}(x)\rho_i^*(x)+\int_\Gamma\rho_i^*(x_0)F_{ij}(x_0,x)R_0\,\mathrm{d}s_0,\quad x\in\Gamma \tag{6}$$

where ρ_i^* in this case can be interpreted as the fictitious source density distributed on Γ. Substituting eqn (6) into (5) and using (4) for x_0 in Ω, the following boundary integral identity is obtained:

$$\int_\Gamma\{u_jt_j^*(\mathbf{u}^*)-t_j(\mathbf{u})u_j^*\}R\,\mathrm{d}s=0. \tag{7}$$

This identity corresponds to Betti's reciprocal theorem for two arbitrary equilibrium states [Timoshenko and Goodier (1970)]: one with u_i and t_i, and the other with u_i^* and t_i^*. Although the identity (7) was used to derive the adjoint system in the adjoint variable method by Lee and Kwak (1992), it will be used in this paper to derive a new BIE for direct calculation of design derivatives.

METHOD OF SDSA

Based on the BIE formulation in the previous section, the direct differentiation method for the SDSA of axisymmetric elastic solids is now presented. The material derivative as shown in Haug *et al.* (1986) is taken to the boundary integral identity (7). After some manipulations and simplifications, the resulting equation can be written as

$$\int_\Gamma (\dot{u}_j t_j^* - \dot{t}_j u_j^*) R \,\mathrm{d}s$$

$$= \int_\Gamma [-(\sigma_{ji} V_k e_{ik}) u_{j,s}^* + u_{j,i} V_i t_j^* + \{t_j (V_{i,s} s_i + V_R/R) - \sigma_{\theta\theta} V_i n_i \delta_{jR}/R\} u_j^*] R \,\mathrm{d}s \quad (8)$$

where $\dot{u}_j$ and $\dot{t}_j$ represent the material derivative, $\mathbf{V} = \{V_R, V_Z\}$ the design velocity vector, s_i the unit tangential vector on the boundary, δ_{ij} the Kronecker delta and

$$[e_{ik}] = \begin{bmatrix} 0 & -1 \\ 1 & 0 \end{bmatrix}. \quad (9)$$

Since u_j^* and t_j^* are defined in the form of the indirect BIE (6), $u_{j,s}^*$ in eqn (8) can be expressed as

$$u_{j,s}^*(x) = d_{ij}(x)\rho_i^*(x) + \int_\Gamma \rho_i^*(x_0) P_{ij}(x_0, x) R_0 \,\mathrm{d}s_0, \quad x \in \Gamma \quad (10)$$

where the coefficient d_{ij} appears as a result of the singularity of the kernel $P_{ij}(x_o, x)$ when the source point x_o coincides with the field point x. The new kernel P_{ij} can be derived by taking a tangential derivative to the kernel G_{ij}, as

$$P_{ij}(x_0, x) \equiv G_{ij,s}(x_0, x) = G_{ij,k}(x_0, x) s_k(x) \quad (11)$$

$G_{ij,k}$ is described in Appendix A. Substituting u_j^*, t_j^* and $u_{j,s}^*$ of the indirect BIEs (6) and (10) into (8) and enforcing that the resulting equation holds for arbitrary source density ρ_i^* on the boundary, the following BIE for the material derivatives of displacement and surface traction is obtained.

$$c_{ij}^0 \dot{u}_j^0 + \int_\Gamma (\dot{u}_j F_{ij} - \dot{t}_j G_{ij}) R \,\mathrm{d}s = -d_{ij}^0 (\sigma_{jk} V_l e_{kl})^0 - \int_\Gamma (\sigma_{jk} V_l e_{kl}) P_{ij} R \,\mathrm{d}s + c_{ij}^0 (u_{j,k} V_k)^0$$

$$+ \int_\Gamma (u_{j,k} V_k) F_{ij} R \,\mathrm{d}s + \int_\Gamma \{t_j (V_{k,s} s_k + V_R/R) - \sigma_{\theta\theta} V_k n_k \delta_{jR}/R\} G_{ij} R \,\mathrm{d}s, \quad x_0 \in \Gamma \quad (12)$$

where the arguments x_0 and x are omitted for simplicity and the superscript 0 represents the value at x_0. Although this equation looks very complicated, it is seen that it can be obtained by simply replacing u_j^*, t_j^* and $u_{j,s}^*$ in eqn (8) by G_{ij}, F_{ij} and P_{ij}, respectively, and that the coefficients c_{ij}^0 and d_{ij}^0 appear from singularity of the kernels.

It is observed that strong singularity of order $O(l/r)$ arises by the kernels F_{ij} and P_{ij} in numerical integration. The singular integration from the kernel F_{ij} can be avoided by use of modes of deformation. Because a rigid body translation in the Z direction gives zero surface traction ($u_R = 0, u_Z = 1, t_R = t_Z = 0$), we obtain from boundary integral identity (7)

$$\int_\Gamma t_Z^* R \,\mathrm{d}s = 0. \tag{13}$$

For an inflation mode in the R direction, displacements and surface tractions become [Bakr (1986)]

$$u_R = R, \quad u_Z = 0, \quad t_R = 2(\lambda+\mu)n_R, \quad t_Z = 2\lambda n_Z \tag{14}$$

and the boundary integral identity (7) becoming

$$\int_\Gamma \{Rt_R^* - 2(\lambda+\mu)n_R u_R^* - 2\lambda n_Z u_Z^*\} R \,\mathrm{d}s = 0. \tag{15}$$

Now substituting indirect BIE expression (6) into eqns (13) and (15) and enforcing that the resulting equation hold for arbitrary source density ρ_i^* on the boundary, the following equations can be obtained:

$$\begin{aligned} &c_{iZ}^0 + \int_\Gamma F_{iZ} R \,\mathrm{d}s = 0 \\ &c_{iR}^0 + \int_\Gamma F_{iR} R \,\mathrm{d}s = \frac{1}{R_0}\int_\Gamma [2\{(\lambda+\mu)n_R\,\delta_{jR} + \lambda n_Z\,\delta_{jZ}\}G_{ij} - F_{iR}(R-R_0)]R\,\mathrm{d}s, \quad x_0 \in \Gamma. \end{aligned} \tag{16}$$

Multiplying the first and the second equations of (16) by $(u_{Z,k}V_k)^0$ and $(u_{R,k}V_k)^0$, respectively, and summing the resulting two equations, the following equation can be obtained:

$$\begin{aligned} &c_{ij}^0(u_{j,k}V_k)^0 + (u_{j,k}V_k)^0 \int_\Gamma F_{ij} R \,\mathrm{d}s \\ &\quad = \frac{(u_{R,k}V_k)^0}{R_0}\int_\Gamma [2\{(\lambda+\mu)n_R\,\delta_{jR} + \lambda n_Z\,\delta_{jZ}\}G_{ij} - (R-R_0)\,\delta_{jR}F_{ij}]R\,\mathrm{d}s, \quad x_0 \in \Gamma. \end{aligned} \tag{17}$$

On the other hand, the singular term including the kernel P_{ij} can be avoided by use of the uniqueness of displacement as

$$\int_\Gamma \mathrm{d}(u_j^* R) = 0 = \int_\Gamma (u_j^* R)_{,s}\,\mathrm{d}s = \int_\Gamma (u_{j,s}^* R + u_j^* s_R)\,\mathrm{d}s. \tag{18}$$

Substituting indirect BIE expressions (6) and (10) into the above equation and taking similar operations as for the term of the kernel F_{ij}, the following equation can be obtained:

$$d_{ij}^0(\sigma_{jk}V_l e_{kl})^0 + (\sigma_{jk}V_l e_{kl})^0 \int_\Gamma P_{ij} R \,\mathrm{d}s = -(\sigma_{jk}V_l e_{kl})^0 \int_\Gamma G_{ij} s_R \,\mathrm{d}s, \quad x_0 \in \Gamma. \tag{19}$$

If eqns (17) and (19) are substituted into (12), then the following new BIE for shape sensitivity is obtained:

$$c_{ij}^0 \dot{u}_j^0 + \int_\Gamma (\dot{u}_j F_{ij} - \dot{t}_j G_{ij}) R \, ds$$

$$= \int_\Gamma [-(A_j - A_j^0) P_{ij} + \{(B_j - B_j^0) - \delta_{jR} B_R^0 (R - R_0)/R_0\} F_{ij} + C_j G_{ij}] R \, ds, \quad x_0 \in \Gamma \tag{20}$$

where

$$A_j = \sigma_{jk} V_l e_{kl}$$
$$B_j = u_{j,k} V_k$$
$$C_j = t_j (V_{k,s} s_k + V_R/R) + A_j^0 s_R/R + 2B_R^0/R_0 \{(\lambda + \mu) n_R \delta_{jR} + \lambda n_Z \delta_{jZ}\} - \sigma_{\theta\theta} V_k n_k \delta_{jR}/R. \tag{21}$$

Because the order of $(A_j - A_j^0)$, $(B_j - B_j^0)$ and $(R - R_0)$ are $O(r)$, the first two integral operators in the right-hand side of eqn (20) are regular. Thus singularity problem is avoided and standard Gaussian quadrature can be employed for the numerical integration. The integral operators in the left-hand side of eqn (20) are the same as those of the original direct BIE (4). Hence, only the right-hand side integrals can be calculated for sensitivity analysis. Representing the design boundary ϕ by a set of shape parameters b_i, the design velocity and the material derivatives of displacements and surface tractions are expressed as

$$\mathbf{V} = \frac{\partial \phi}{\partial b_j} \delta b_j, \quad \dot{u}_i = \frac{\partial u_i}{\partial b_j} \delta b_j, \quad \dot{t}_i = \frac{\partial t_i}{\partial b_j} \delta b_j. \tag{22}$$

If eqn (22) is substituted into (20) and (21), then the sensitivities of displacements and surface tractions in terms of the shape parameters, i.e., design variables can be directly solved by implementation of the BEM.

In numerical implementation of the shape optimization problem, stress sensitivities are usually required. Once the displacement and traction sensitivities are calculated, the sensitivities of the various stresses arising in the axisymmetric elasticity problem can be calculated by formulas as described in Appendix B.

NUMERICAL EXAMPLES

Three axisymmetric example problems are treated for numerical implementation of the presented method of the SDSA. Predicted sensitivities are compared with analytic sensitivities if available and with those by finite differences if not. Numerical calculation is performed on the SGI Indigo R3000 engineering workstation. Quadratic boundary elements are used for the implementation of the BIE. For all examples, Young's modulus and Poisson's ratio are set as 30×10^6 psi and 0.3, respectively.

A hollow disk under uniform external tensile load

The first example is a hollow disk under uniform tensile load on the outer surface. It is the same example that was treated by Saigal *et al.* (1989) implementing implicit differentiation methods. Analytic solution is given by Timoshenko and Goodier (1970). The inner radius r_1, outer radius r_2 and thickness of the disk are set as 4, 20 and 2 inches, respectively. The magnitude of the tensile load is 1,000 psi. The inner radius r_1 is taken as

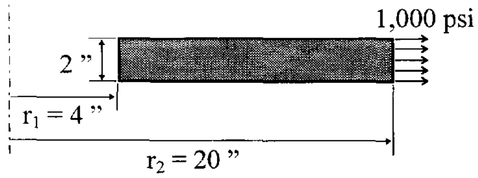

Fig. 2. A hollow disk under uniform external tensile load.

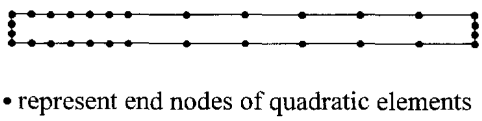

Fig. 3. A quadratic boundary element model for the hollow disk problem.

the design variable. The exact sensitivity expression in terms of the design variable has been shown by Kane and Saigal (1988).

The disk is discretized by thirty elements as shown in Fig. 3, which is the same mesh configuration as used by Saigal *et al.* (1989). The predicted displacement sensitivities by the present method are listed in Table 1 and are compared with those by analytic sensitivities and by Saigal *et al.* (1989). It is observed that very accurate results are obtained and the degree of accuracy of present method is as high as Saigal *et al.* (1989) for this example.

A thick-walled cylinder under internal and external pressure

A thick-walled cylinder problem as shown in Fig. 4 is considered here. The inner radius r_1 and outer radius r_2 are set as 10 and 20 inches, respectively. Uniform pressure of 1,000 and 500 psi are applied on the internal and external surface. Analytic solution is also given by Timoshenko and Goodier (1970). The outer radius r_2 is taken as the design variable for the current example. Analytic sensitivities of displacement, hoop stress and radial stress in terms of the outer radius r_2 can be derived as follows:

Table 1. Displacement sensitivities of the hollow disk problem

Radius	Analytic	Saigal *et al.* (1989)	Present
4.0	0.75231E−04	0.75228E−04	0.75226E−04
4.3	0.75139E−04	0.75135E−04	0.74916E−04
4.7	0.74480E−04	0.74475E−04	0.74806E−04
5.0	0.73466E−04	0.73462E−04	0.73334E−04
5.3	0.72235E−04	0.72231E−04	0.72411E−04
5.7	0.70875E−04	0.70871E−04	0.70795E−04
6.0	0.69444E−04	0.69440E−04	0.69546E−04
6.3	0.67982E−04	0.67978E−04	0.67930E−04
6.7	0.66512E−04	0.66508E−04	0.66573E−04
7.0	0.65054E−04	0.65050E−04	0.65017E−04
7.3	0.63618E−04	0.63614E−04	0.63651E−04
7.7	0.62210E−04	0.62206E−04	0.62178E−04
8.0	0.60836E−04	0.60833E−04	0.60935E−04
9.0	0.56933E−04	0.56930E−04	0.56848E−04
10.0	0.53356E−04	0.53354E−04	0.53444E−04
11.0	0.50081E−04	0.50078E−04	0.50042E−04
12.0	0.47068E−04	0.47065E−04	0.47099E−04
13.0	0.44282E−04	0.44279E−04	0.44264E−04
14.0	0.41690E−04	0.41688E−04	0.41700E−04
15.0	0.39265E−04	0.39263E−04	0.39255E−04
16.0	0.36983E−04	0.36980E−04	0.36984E−04
17.0	0.34824E−04	0.34821E−04	0.34817E−04
18.0	0.32772E−04	0.32769E−04	0.32766E−04
19.0	0.30813E−04	0.30810E−04	0.30808E−04
20.0	0.28935E−04	0.28933E−04	0.28930E−04

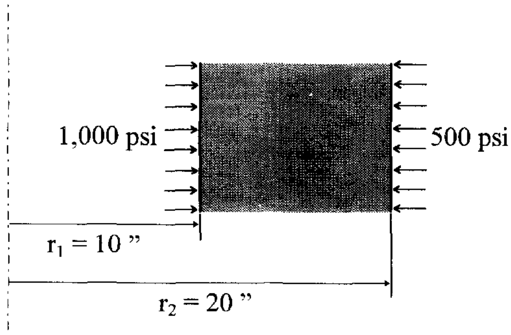

Fig. 4. A thick-walled cylinder under internal and external pressure.

$$\frac{\mathrm{d}u_R}{\mathrm{d}r_2}=\frac{\partial u_R}{\partial r_2}+\frac{\partial u_R}{\partial R}\frac{\mathrm{d}R}{\mathrm{d}r_2},\quad \frac{\mathrm{d}\sigma_{\theta\theta}}{\mathrm{d}r_2}=\frac{\partial \sigma_{\theta\theta}}{\partial r_2}+\frac{\partial \sigma_{\theta\theta}}{\partial R}\frac{\mathrm{d}R}{\mathrm{d}r_2},\quad \frac{\mathrm{d}\sigma_{RR}}{\mathrm{d}r_2}=\frac{\partial \sigma_{RR}}{\partial r_2}+\frac{\partial \sigma_{RR}}{\partial R}\frac{\mathrm{d}R}{\mathrm{d}r_2}$$

where

$$\frac{\mathrm{d}R}{\mathrm{d}r_2}=\frac{R-r_1}{r_2-r_1} \tag{23}$$

and partial derivatives of u_R, $\sigma_{\theta\theta}$ and θ_{RR} with respect to r_2 and R can be obtained by differentiating analytic solution.

Thirty boundary elements are used to model the cylinder, as shown in Fig. 5. The sensitivities analyzed by the present method of the SDSA are listed in Table 2 and are compared with analytic sensitivities. Very accurate results are shown. The worst accuracy for the radial stress sensitivities arises in the neighborhood of the internal and external surface, but it is trivial because it occurs on the boundary with sensitivities of relatively small magnitude.

A spherical vessel with a nozzle

The final example is a spherical pressure vessel with a nozzle, as shown in Fig. 6. Internal pressure is set as 10,000 psi. Inner radius r_1 is defined as the design variable. The spherical vessel is discretized by thirty-two quadratic elements, as shown in Fig. 7.

Generally, von Mises effective stress can be used for a stress constraint criterion in the shape optimization problem. Hence, sensitivities of von Mises effective stresses are considered for the current example. Because analytic solution is not available, predicted sensitivities are compared with those by finite differences. In the method of finite differences, 0.1 per cent change of the design variable is used for the numerical differentiation. Listed in Table 3 are sensitivities of von Mises effective stresses at the nodes on the external surface. The maximum error is 9.75 per cent relative to the method of finite differences. It is seen that the overall accuracy is very favorable.

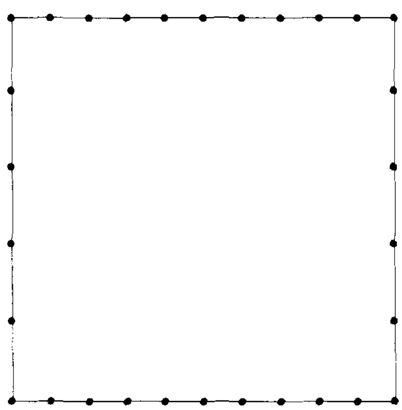

Fig. 5. A quadratic boundary element model for the thick-walled cylinder problem.

Table 2. Sensitivities of the thick-walled cylinder problem

Radius	Displacement sensitivities Analytic	Displacement sensitivities Present	Hoop stress sensitivities Analytic	Hoop stress sensitivities Present	Radial stress sensitivities Analytic	Radial stress sensitivities Present
10.0	−0.13481E−04	−0.13482E−04	−0.44444E+02	−0.44446E+02	0.00000E+00	−0.37152E+01
10.5	−0.14815E−04	−0.14817E−04	−0.48137E+02	−0.48078E+02	0.36929E+01	0.38834E+01
11.0	−0.15957E−04	−0.15943E−04	−0.50605E+02	−0.50748E+02	0.61608E+01	0.56915E+01
11.5	−0.16947E−04	−0.16953E−04	−0.52176E+02	−0.52206E+02	0.77313E+01	0.76058E+01
12.0	−0.17815E−04	−0.17801E−04	−0.53086E+02	−0.53160E+02	0.86420E+01	0.84366E+01
12.5	−0.18585E−04	−0.18593E−04	−0.53511E+02	−0.53517E+02	0.90667E+01	0.90419E+01
13.0	−0.19276E−04	−0.19262E−04	−0.53578E+02	−0.53624E+02	0.91337E+01	0.90126E+01
13.5	−0.19903E−04	−0.19911E−04	−0.53383E+02	−0.53389E+02	0.89383E+01	0.89097E+01
14.0	−0.20478E−04	−0.20463E−04	−0.52996E+02	−0.53029E+02	0.85520E+01	0.84774E+01
14.5	−0.21009E−04	−0.21017E−04	−0.52473E+02	−0.52479E+02	0.80282E+01	0.79986E+01
15.0	−0.21506E−04	−0.21492E−04	−0.51852E+02	−0.51876E+02	0.74074E+01	0.73598E+01
15.5	−0.21974E−04	−0.21982E−04	−0.51165E+02	−0.51171E+02	0.67202E+01	0.66911E+01
16.0	−0.22419E−04	−0.22406E−04	−0.50434E+02	−0.50453E+02	0.59896E+01	0.59575E+01
16.5	−0.22845E−04	−0.22852E−04	−0.49678E+02	−0.49684E+02	0.52332E+01	0.52039E+01
17.0	−0.23254E−04	−0.23243E−04	−0.48909E+02	−0.48923E+02	0.44643E+01	0.44414E+01
17.5	−0.23652E−04	−0.23658E−04	−0.48137E+02	−0.48147E+02	0.36929E+01	0.36610E+01
18.0	−0.24038E−04	−0.24029E−04	−0.47371E+02	−0.47360E+02	0.29264E+01	0.29198E+01
18.5	−0.24417E−04	−0.24424E−04	−0.46615E+02	−0.46568E+02	0.21703E+01	0.24410E+01
19.0	−0.24789E−04	−0.24770E−04	−0.45873E+02	−0.45820E+02	0.14288E+01	0.14244E+01
19.5	−0.25156E−04	−0.25164E−04	−0.45149E+02	−0.45380E+02	0.70466E+00	−0.14596E+00
20.0	−0.25519E−04	−0.25527E−04	−0.44444E+02	−0.44434E+02	0.00000E+00	−0.63633E+01

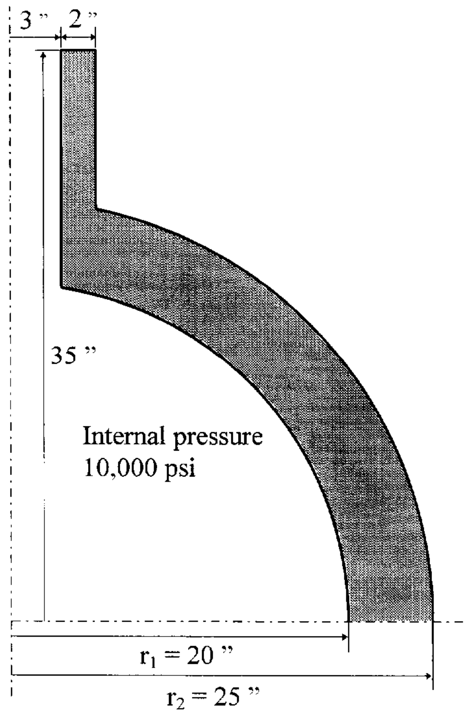

Fig. 6. A spherical vessel with a nozzle.

CONCLUSION

A new direct differentiation method of the SDSA for axisymmetric elastic solids is presented based on the boundary integral formulation and numerically implemented. The present paper completes the concept of the unified adjoint and direct approach using the axisymmetric BIE formulation. In general, selection from the direct and adjoint methods depends on the numbers of the design variables and the objective and constraint functions of the optimization problem under consideration. From the viewpoint of the numerical calculation, the present direct method gives a clear advantage over the adjoint method. It results from the fact that the current method avoids the singular boundary condition which

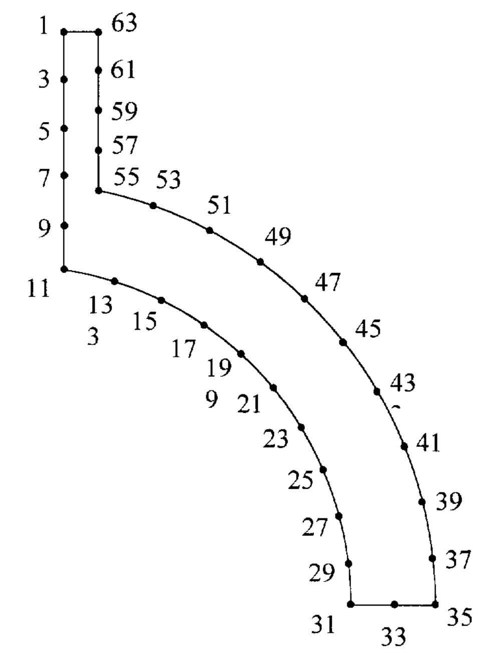

Fig. 7. A quadratic boundary element model and node numbers for the spherical vessel problem.

Table 3. Effective stress sensitivities of the spherical vessel problem

Node	Finite difference	Present	Ratio (%)*
35	0.47688E+04	0.47049E+04	100.91
36	0.47831E+04	0.47583E+04	99.48
37	0.48162E+04	0.47787E+04	99.22
38	0.48486E+04	0.48031E+04	99.06
39	0.48723E+04	0.48273E+04	99.08
40	0.48892E+04	0.48487E+04	99.17
41	0.48998E+04	0.48657E+04	99.30
42	0.49059E+04	0.48792E+04	99.46
43	0.49079E+04	0.48893E+04	99.62
44	0.49077E+04	0.48973E+04	99.79
45	0.49068E+04	0.49041E+04	99.95
46	0.49064E+04	0.49098E+04	100.07
47	0.49087E+04	0.49151E+04	100.13
48	0.49134E+04	0.49178E+04	100.09
49	0.49226E+04	0.49176E+04	99.90
50	0.49319E+04	0.49069E+04	99.49
51	0.49377E+04	0.48770E+04	98.77
52	0.49152E+04	0.47909E+04	97.47
53	0.48583E+04	0.46145E+04	94.98
54	0.49125E+04	0.44826E+04	91.25
55	0.42281E+04	0.43774E+04	103.53

* Ratio means a percentage value of (Present)/(Finite difference).

might occur when sensitivities at nodal points are to be found by the adjoint method. Theoretical formulation is validated through three numerical examples. An implementation for a practical shape optimization problem is under study to show realistic application of present work.

REFERENCES

Bakr, A. A. (1986). *The Boundary Integral Equation Method in Axisymmetric Stress Analysis Problems*, Springer-Verlag, Berlin.

Banerjee, P. K. and Butterfield, R. (1981). *Boundary Element Methods in Engineering Science*, McGraw-Hill, New York.

Barone, M. R. and Yang, R. J. (1988). Boundary integral equations for recovery of design sensitivities in shape optimization. *AIAA J.* **26**, 589–594.

Barone, M. R. and Yang, R. J. (1989). A boundary element approach for recovery of shape sensitivities in three-dimensional elastic solids. *Comp. Meth. Appl. Mech. Engng* **74**, 69–82.

Brebbia, C. A., Telles, J. C. F. and Wrobel, L. C. (1984). *Boundary Element Techniques*, Springer-Verlag, Berlin.

Burczynski, T. (1993). Recent advances in boundary element approach to design sensitivity analysis—a survey. In *Design-Sensitivity Analysis* (eds M. Kleiber and T. Hisada). Atlanta Technology Publications, Atlanta.

Chen, C.-J. and Choi, K. K. (1994). Continuum approach for second-order shape design sensitivity of three-dimensional elastic solids. *AIAA J.* **32**, 2099–2107.

Choi, J. H. and Choi, K. K. (1990). Direct differentiation method for shape design sensitivity analysis using boundary integral formulation. *Comput. Struct.* **34**, 499–508.

Choi, J. H. and Kwak, B. M. (1988). Boundary integral equation method for shape optimization of elastic structures. *Int. J. Num. Meth. Engng* **26**, 1579–1595.

Choi, J. H. and Kwak, B. M. (1990). A unified approach for adjoint and direct method in shape design sensitivity analysis using boundary integral formulation. *Engng Anal. Boundary Elements* **7**, 39–45.

Haug, E. J., Choi, K. K. and Komkov, V. (1986). *Design Sensitivity Analysis of Structural Systems*, Academic Press, New York.

Kane, J. H. and Saigal, S. (1988). Design sensitivity analysis of solids using BEM. *J. Engng Mech.* **114**, 1703–1722.

Lee, B. Y. and Kwak, B. M. (1991). Shape optimization of two-dimensional thermoelastic structures using boundary integral equation formulation. *Comput. Struct.* **41**, 709–722.

Lee, B. Y. and Kwak, B. M. (1992). Axisymmetric thermoelastic shape sensitivity analysis and its application to turbine disc design. *Int. J. Num. Meth. Engng* **33**, 2073–2089.

Mota Soares, C. A., Rodrigues, H. C. and Choi, K. K. (1984). Shape optimal structure design using boundary elements minimum compliance techniques. *J. Mech. Trans. Automa. Des. ASME* **106**, 518–523.

Rice, J. S. and Mukherjee, S. (1990). Design sensitivity coefficients for axisymmetric elasticity problems by boundary element methods. *Engng Anal. Boundary Elements* **7**, 13–20.

Saigal, S., Borggaard, J. T. and Kane, J. H. (1989). Boundary element implicit differentiation equations for design sensitivities of axisymmetric structures. *Int. J. Solids Structures* **25**, 527–538.

Timoshenko, S. P. and Goodier, J. N. (1970). *Theory of Elasticity*, 3rd edn, McGraw-Hill, New York.

APPENDIX A

$G_{ij,k}$ in eqn (11) is expressed as follows:

$$G_{RR,R}=\frac{A}{R_0R^2(a+b)}\Bigg[2(3-4v)R^2\sqrt{a+b}K+\{(3-4v)(R^2+R_0^2)+4(1-v)\bar{Z}^2\}$$

$$\times\left\{K_{,R}R\sqrt{a+b}-K\left(\sqrt{a+b}+\frac{R(R+R_0)}{\sqrt{a+b}}\right)\right\}-\left\{2(3-4v)(R+R_0)+\frac{2\bar{Z}^2(R_0a-Rb)}{(a-b)^2}\right\}$$

$$\times ER\sqrt{a+b}-\left\{(3-4v)(a+b)+\frac{\bar{Z}^2a}{a-b}\right\}\left\{E_{,R}R\sqrt{a+b}-E\left(\sqrt{a+b}+\frac{R(R+R_0)}{\sqrt{a+b}}\right)\right\}\Bigg]$$

$$G_{RR,Z}=\frac{A}{RR_0(a+b)}\Bigg[8(1-v)\bar{Z}\sqrt{a+b}K+\left\{(3-4v)(R^2+R_0^2)+4(1-v)\bar{Z}^2\right\}$$

$$\times\left(K_{,Z}\sqrt{a+b}-K\frac{\bar{Z}}{\sqrt{a+b}}\right)-\left\{2(3-4v)\bar{Z}+\frac{2\bar{Z}(a^2-ab-\bar{Z}^2\cdot b)}{(a-b)^2}\right\}E\sqrt{a+b}$$

$$-\left\{(3-4v)(a+b)+\frac{\bar{Z}^2a}{a-b}\right\}\left(E_{,Z}\sqrt{a+b}-E\frac{\bar{Z}}{\sqrt{a+b}}\right)\Bigg]$$

$$G_{RZ,R}=\frac{A\bar{Z}}{R_0(a+b)}\Bigg[-K_{,R}\sqrt{a+b}+K\frac{R+R_0}{\sqrt{a+b}}+\frac{2\{R(a-b)-(R^2-R_0^2+\bar{Z}^2)(R-R_0)\}}{(a-b)^2}E\sqrt{a+b}$$

$$+\frac{R^2-R_0^2+\bar{Z}^2}{a-b}\left(E_{,R}\sqrt{a+b}-E\frac{R+R_0}{\sqrt{a+b}}\right)\Bigg]$$

$$G_{RZ,Z}=\frac{A}{R_0(a+b)}\Bigg[-K\sqrt{a+b}-\bar{Z}\left(K_{,Z}\sqrt{a+b}-K\frac{\bar{Z}}{\sqrt{a+b}}\right)$$

$$+\frac{(R^2-R_0^2+3\bar{Z}^2)(a-b)-2\bar{Z}^2(R^2-R_0^2+\bar{Z}^2)}{(a-b)^2}E\sqrt{a+b}$$

$$+\frac{\bar{Z}(R^2-R_0^2+\bar{Z}^2)}{a-b}\left(E_{,Z}\sqrt{a+b}-E\frac{\bar{Z}}{\sqrt{a+b}}\right)\Bigg]$$

$$G_{ZR,R}=\frac{A\bar{Z}}{R^2(a+b)}\Bigg[K_{,R}R\sqrt{a+b}-K\left(\sqrt{a+b}+\frac{R(R+R_0)}{\sqrt{a+b}}\right)$$

$$+\frac{2\{R(a-b)+(R_0^2-R^2+\bar{Z}^2)(R-R_0)\}}{(a-b)^2}ER\sqrt{a+b}$$

$$-\frac{R_0^2-R^2+\bar{Z}^2}{a-b}\left\{E_{,R}R\sqrt{a+b}-E\left(\sqrt{a+b}+\frac{R(R+R_0)}{\sqrt{a+b}}\right)\right\}\Bigg]$$

$$G_{ZR,Z}=\frac{A}{R(a+b)}\Bigg[K\sqrt{a+b}+\bar{Z}\left(K_{,Z}\sqrt{a+b}-K\frac{\bar{Z}}{\sqrt{a+b}}\right)$$

$$-\frac{(R_0^2-R^2+3\bar{Z}^2)(a-b)-2\bar{Z}^2(R_0^2-R^2+\bar{Z}^2)}{(a-b)^2}E\sqrt{a+b}$$

$$-\frac{\bar{Z}(R_0^2-R^2+\bar{Z}^2)}{a-b}\left(E_{,Z}\sqrt{a+b}-E\frac{\bar{Z}}{\sqrt{a+b}}\right)\Bigg]$$

$$G_{ZZ,R}=\frac{2A}{a+b}\Bigg[(3-4v)\left(K_{,R}\sqrt{a+b}-K\frac{R+R_0}{\sqrt{a+b}}\right)-\frac{2\bar{Z}^2(R-R_0)}{(a-b)^2}E\sqrt{a+b}$$

$$+\frac{\bar{Z}^2}{a-b}\left(E_{,R}\sqrt{a+b}-E\frac{R+R_0}{\sqrt{a+b}}\right)\Bigg]$$

$$G_{ZZ,Z}=\frac{2A}{a+b}\Bigg[(3-4v)\left(K_{,Z}\sqrt{a+b}-K\frac{\bar{Z}}{\sqrt{a+b}}\right)+\frac{2\bar{Z}(a-b)-2\bar{Z}^3}{(a-b)^2}E\sqrt{a+b}$$

$$+\frac{\bar{Z}^2}{a-b}\left(E_{,Z}\sqrt{a+b}-E\frac{\bar{Z}}{\sqrt{a+b}}\right)\Bigg]$$

where ν denotes Poisson's ratio and

$$\bar{Z} = Z-Z_0,\quad a = R^2+R_0^2+\bar{Z}^2,\quad b = 2RR_0,\quad A = \frac{1}{8\pi\mu(1-\nu)}$$

K and E denote the first and the second kind of complete elliptic integral, respectively, as

$$K(m) = \int_0^{\pi/2}(1-m\sin^2\xi)^{-1/2}\,d\xi,\quad E(m) = \int_0^{\pi/2}(1-m\sin^2\xi)^{1/2}\,d\xi$$

where

$$m = \frac{2b}{a+b}.$$

Derivatives of K and E are expressed as

$$K_{,R} = \frac{2(R_0a-Rb)}{(a+b)^2}\left\{\frac{E}{1-m}-\frac{K-E}{m}\right\}$$

$$K_{,Z} = -\frac{2b\bar{Z}}{(a+b)^2}\left\{\frac{E}{1-m}-\frac{K-E}{m}\right\}$$

$$E_{,R} = -\frac{2(R_0a-Rb)}{(a+b)^2}\left\{K-\frac{E-(1-m)K}{m}\right\}$$

$$E_{,Z} = \frac{2b\bar{Z}}{(a+b)^2}\left\{K-\frac{E-(1-m)K}{m}\right\}.$$

APPENDIX B

Various stress components on the boundary can be expressed in terms of the displacements and tractions as follows:

$$\sigma_{nn} = \sigma_{ij}n_in_j = t_in_i$$

$$\sigma_{ns} = \sigma_{ij}n_is_j = t_is_i$$

$$\sigma_{ss} = \sigma_{ij}s_is_j = C_1\varepsilon_{ss}+C_2\varepsilon_{\theta\theta}+C_3\sigma_{nn}$$

$$\sigma_{RR} = \sigma_{nn}n_R^2+\sigma_{ss}n_Z^2-2\sigma_{ns}n_Rn_Z$$

$$\sigma_{ZZ} = \sigma_{nn}n_Z^2+\sigma_{ss}n_R^2+2\sigma_{ns}n_Rn_Z$$

$$\sigma_{\theta\theta} = C_1\varepsilon_{\theta\theta}+C_2\varepsilon_{ss}+C_3\sigma_{nn}$$

where

$$\varepsilon_{ss} = u_{i,s}s_i$$

and

$$C_1 = \frac{2\mu}{1-\nu},\quad C_2 = \frac{2\mu\nu}{1-\nu},\quad C_3 = \frac{\nu}{1-\nu}.$$

Von Mises effective stress can be expressed, considering the axisymmetry, as

$$\sigma_e = (\sigma_{nn}^2+\sigma_{ss}^2+\sigma_{\theta\theta}^2+3\sigma_{ns}^2-\sigma_{nn}\sigma_{ss}-\sigma_{nn}\sigma_{\theta\theta}-\sigma_{\theta\theta}\sigma_{ss})^{1/2}.$$

Once the state variables and their shape sensitivities are obtained, sensitivities of the various stress components on the boundary can be calculated by the following formulae:

$$\dot{\sigma}_{nn} = \dot{t}_in_i+t_i\dot{n}_i$$

$$\dot{\sigma}_{ns} = \dot{t}_is_i+t_i\dot{s}_i$$

$$\dot{\sigma}_{ss} = C_1\dot{\varepsilon}_{ss}+C_2\dot{\varepsilon}_{\theta\theta}+C_3\dot{\sigma}_{nn}$$

$$\dot{\sigma}_{RR} = \dot{\sigma}_{nn}n_R^2+\dot{\sigma}_{ss}n_Z^2-2\dot{\sigma}_{ns}n_Rn_Z+2\sigma_{nn}n_R\dot{n}_R+2\sigma_{ss}n_Z\dot{n}_Z-2\sigma_{ns}(n_R\dot{n}_Z+n_Z\dot{n}_R)$$

$$\dot{\sigma}_{ZZ} = \dot{\sigma}_{nn}n_Z^2 + \dot{\sigma}_{ss}n_R^2 + 2\dot{\sigma}_{ns}n_R n_Z + 2\sigma_{nn}n_Z\dot{n}_Z + 2\sigma_{ss}n_R\dot{n}_R + 2\sigma_{ns}(n_R\dot{n}_Z + n_Z\dot{n}_R)$$

$$\dot{\sigma}_{\theta\theta} = C_1\dot{\varepsilon}_{\theta\theta} + C_2\dot{\varepsilon}_{ss} + C_3\dot{\sigma}_{nn}$$

$$\dot{\sigma}_e = \frac{1}{2\sigma_e}\{2(\sigma_{nn}\dot{\sigma}_{nn} + \sigma_{ss}\dot{\sigma}_{ss} + \sigma_{\theta\theta}\dot{\sigma}_{\theta\theta}) - \sigma_{nn}\dot{\sigma}_{ss} - \sigma_{ss}\dot{\sigma}_{nn} - \sigma_{nn}\dot{\sigma}_{\theta\theta} - \sigma_{\theta\theta}\dot{\sigma}_{nn}$$

$$- \sigma_{ss}\dot{\sigma}_{\theta\theta} - \sigma_{\theta\theta}\dot{\sigma}_{ss} + 6\sigma_{ns}\dot{\sigma}_{ns}\}$$

where $\dot{n}_i$ and $\dot{s}_i$ represent the material derivatives of the normal and tangential unit vectors, respectively, which can be expressed as follows:

$$\dot{n}_i = (V_s H - V_{n,s})s_i$$

$$\dot{s}_i = (V_{n,s} - V_s H)n_i.$$

Here V_n and V_s represent the normal and tangential components of the design velocity, and H means the curvature of the boundary. The material derivatives of the strains can be expressed as

$$\dot{\varepsilon}_{ss} = \dot{u}_{i,s}s_i + u_{i,s}n_i(V_{n,s} - V_s H) - \varepsilon_{ss}(V_n H + V_{s,s})$$

$$\dot{\varepsilon}_{\theta\theta} = \frac{1}{R}\{\dot{u}_R - \varepsilon_{\theta\theta}(n_R V_n - n_Z V_s)\}.$$